

1 Partitioning of canopy and soil CO₂ fluxes in a pine forest at the dry 2 timberline across a 13-year observation period

3 Rafat Qubaja^a, Fyodor Tatarinov^a, Eyal Rotenberg^a, and Dan Yakir^{a*}

4 ^a Department of Earth and Planetary Sciences, Weizmann Institute of Science, Rehovot 76100, Israel

5 *Correspondence: Dan Yakir; email: dan.yakir@weizmann.ac.il

6 Abstract

7 Partitioning carbon fluxes is key to understanding the process underlying ecosystem response to change.
8 This study used soil and canopy fluxes with stable isotopes (¹³C) and radiocarbon (¹⁴C) measurements in
9 an 18 km², 50-year-old dry (287 mm mean annual precipitation; non-irrigated) *Pinus halepensis* forest
10 plantation in Israel to partition the net ecosystem's CO₂ flux into gross primary productivity (GPP) and
11 ecosystem respiration (Re) and (with the aid of isotopic measurements) soil respiration flux (Rs) into
12 autotrophic (Rsa), heterotrophic (Rh), and inorganic (Ri) components. On an annual scale, GPP and Re
13 were 655 and 488 g C m⁻², respectively, with a net primary productivity (NPP) of 282 g C m⁻² and carbon-
14 use efficiency (CUE=NPP/GPP) of 0.43. Rs made up 60% of the Re and comprised 24 ± 4%, 23 ± 4%, and
15 13 ± 1% from Rsa, Rh, and Ri, respectively. The contribution of root and microbial respiration to Re
16 increased during high productivity periods, and inorganic sources were more significant components when
17 the soil water content was low. Comparing the ratio of the respiration components to Re of our mean 2016
18 values to those of 2003 (mean for 2001–2006) at the same site indicated a decrease in the autotrophic
19 components (roots, foliage, and wood) by about -13%, and an increase in the heterotrophic component
20 (Rh/Re) by about +18%, with similar trends for soil respiration (Rsa/Rs decreasing by -19% and Rh/Rs
21 increasing by +8%, respectively). The soil respiration sensitivity to temperature (Q₁₀) decreased across the
22 same observation period by 36% and 9% in the wet and dry periods, respectively. Low rates of soil carbon
23 loss combined with relatively high belowground carbon allocation (i.e., 38% of canopy CO₂ uptake) and
24 low sensitivity to temperature help explain the high soil organic carbon accumulation and the relatively
25 high ecosystem CUE of the dry forest.

26
27 **Keywords:** Carbon balance, Soil respiration, Autotrophic, Heterotrophic, Inorganic flux, Temperature
28 response, Semi-arid ecosystem, Pine forest, Canopy cover, Soil chamber

29 1. Introduction

30 The annual net storage of carbon in the land biosphere, known as net ecosystem production (NEP), is the
31 balance between carbon uptake during gross primary productivity (GPP) and carbon loss during growth,
32 maintenance respiration by plants (i.e., autotrophic respiration, R_a), and decomposition of litter and soil
33 organic matter (i.e., heterotrophic respiration, R_h ; Bonan, 2008). The difference between GPP and R_a
34 expresses the net primary production (NPP) and is the net carbon uptake by plants that can be used for new
35 biomass production. Measurements from a range of ecosystems have shown that total plant respiration can
36 be as large as 50% of GPP (e.g., Etzold et al., 2011) and together with R_h comprises total ecosystem
37 respiration (R_e , $R_e=R_a+R_h$). The partitioning of the ecosystem carbon fluxes can therefore be summarized
38 as:

$$39 \quad GPP = NPP + R_a = NEP + R_h + R_a \quad (1)$$

40 Earlier campaign-based measurements carried out by Maseyk et al. (2008a) and Grünzweig et al. (2009)
41 in the semi-arid *Pinus halepensis* (Aleppo pine) Yatir forest indicated that GPP at this site was lower than
42 among temperate coniferous forests (1,000–1,900 g C m⁻² y⁻¹) but within the range estimated for
43 Mediterranean evergreen needle-leaf and boreal coniferous forests (Falge et al., 2002; Flechard et al.,
44 2019b), and had a high carbon-use efficiency of 0.4 (CUE = NPP/GPP; DeLucia et al., 2007). The total
45 flux of CO₂ released from the ecosystem (R_e) can be partitioned into aboveground autotrophic respiration
46 (i.e., foliage and sapwood, R_f) and soil CO₂ flux (R_s). R_s , in turn, is a combination of three principal
47 components and can be further partitioned into the components originating from roots or rhizospheres and
48 mycorrhizas (i.e., belowground autotrophic, R_{sa}), from carbon respired during the decomposition of dead
49 organic matter by soil microorganisms and macrofaunal (heterotrophic respiration, R_h ; Bahn et al., 2010;
50 Kuzyakov, 2006), and pedogenic or anthropogenic acidification of soils containing CaCO₃ (R_i ; Joseph et
51 al., 2019; Kuzyakov, 2006), which is expressed as:

$$52 \quad R_e = R_s + R_f = [R_{sa} + R_h + R_i] + R_f \quad (2)$$

53 Previously published results show that the contribution of R_{sa} and R_h to R_s ranges from 24 to 65% and
54 from 29 to 74%, respectively, in forest soils in different biomes and ecosystems (Binkley et al., 2006; Chen
55 et al., 2010; Flechard et al., 2019a; Frey et al., 2006; Hogberg et al., 2009; Subke et al., 2011). Some studies
56 reported significant proportions of abiotic contribution to R_s , ranging between 10 and 60% (Martí-Roura
57 et al., 2019; Ramnarine et al., 2012; Joseph et al., 2019). However, most of these experiments were
58 performed in boreal, temperate, or subtropical forests, and there is a general lack of information on water-
59 limited environments, such as dry Mediterranean ecosystems. Using both ¹³C and CO₂/O₂ ratios also
60 showed that abiotic processes, such as CO₂ storage, transport, and interactions with sediments, can
61 influence R_s measurements at such sites (Angert et al., 2015; Carmi et al., 2013). Furthermore, root-

62 respired CO₂ can also be dissolved in the xylem water and carried upward with the transpiration stream
63 (Etzold et al., 2013).

64 Rates of the soil-atmosphere CO₂ flux (Rs) have been altered owing to global climatic change, particularly
65 through changes in soil temperature (Ts) and soil moisture (SWC; Bond-Lamberty and Thomson, 2010;
66 Buchmann, 2000; Carvalhais et al., 2014; Hagedorn et al., 2016; Zhou et al., 2009), which could account
67 for 65–92% of the variability of Rs in a mixed deciduous forest (Peterjohn et al., 1994). Soil moisture
68 impacts on Rs have been observed in arid and Mediterranean ecosystems, where Ts and SWC are
69 negatively correlated (e.g., Grünzweig et al., 2009). CO₂ efflux generally increases with increasing soil
70 temperatures (Frank et al., 2002), which can produce positive feedback on climate warming (Conant et al.,
71 1998), converting the biosphere from a net carbon sink to a carbon source (IPCC-AR5 2014). A range of
72 empirical models have been developed to relate Rs rate and temperature (Balogh et al., 2011; Lellei-Kovács
73 et al., 2011), and the most widely used models rely on the Q₁₀ approach (Bond-Lamberty and Thomson,
74 2010), which quantifies the sensitivity of Rs to temperature and can integrate it with physical processes,
75 such as the rate of O₂ diffusion into and CO₂ diffusion out of soils and the intrinsic temperature dependency
76 of enzymatic processes (Davidson and Janssens, 2006). Soil moisture (SWC) may be of greater importance
77 than temperature in influencing Rs in water-limited ecosystems (Hagedorn et al., 2016; Grünzweig et al.,
78 2009; Shen et al., 2008). In general, the Rs rate increases with the increase of SWC at low levels but
79 decreases at high levels of SWC (Deng et al., 2012; Hui and Luo, 2004; Jiang et al., 2013). Several studies
80 highlight the sensitivity of carbon fluxes in semi-arid Mediterranean ecosystems to the irregular seasonal
81 and interannual distribution of rain events (Poulter et al., 2014; Ross et al., 2012). While Rs is generally
82 constrained by low SWC during summer months, abrupt and large soil CO₂ pulses have been observed
83 after rewetting the dry soil (Matteucci et al., 2015).

84 The objectives were twofold. First, to obtain detail on partitioning of the carbon fluxes in a semi-arid pine
85 forest to help explain the high productivity and carbon use efficiency recently reported for this ecosystem
86 (Qubaja et al., in press), and provide process-based information to assess the carbon sequestration potential
87 of such a semi-arid afforestation system. Second, to combine this 2016 study with the results of a similar
88 one at the same site in 2003 (mean values for 2001–2006; Grünzweig et al., 2007, 2009) to obtain a long-
89 term perspective across 13 years on soil respiration and its partitioning. We hypothesized that the high
90 carbon use efficiency of the dry forest ecosystem is associated with high belowground carbon allocation
91 and relatively low decomposition rates, and that the long-term trend associated with warming may be
92 suppressed by the dry conditions.

93 **2. Materials and methods**

94 2.1. Site description

95 The Yatir forest (31°20'49" N; 35°03'07" E, 650 m a.s.l.) is situated in the transition zone between sub-
96 humid and arid Mediterranean climates (SI Fig. 1) on the edge of the Hebron mountain ridge. The
97 ecosystem is a semi-arid pine afforestation established in the 1960s and covering approximately 18 km².
98 The average air temperatures for January and July are 10.0 °C and 25.8 °C, respectively. Mean annual
99 potential evapotranspiration (ET) is 1,600 mm, and mean annual precipitation is 287 mm. Only winter
100 (December to March) precipitation occurs in this region, creating a distinctive wet season, while summer
101 (June to October) is an extended dry season. There are short transition periods between seasons, with a
102 wetting season (i.e., autumn) and a drying season (i.e., spring). The forest is dominated by Aleppo pine
103 (*Pinus halepensis* Mill.), with smaller proportions of other pine species and cypress and little understory
104 vegetation. Tree density in 2007 was 300 trees ha⁻¹; mean tree height was 10.0 m; diameter at breast height
105 (DBH) was ~15.9 cm; and the leaf area index (LAI) was ~1.5. The native background vegetation was
106 sparse shrubland, which is dominated by the dwarf shrub *Sarcopoterium spinosum* (L.) Spach, with patches
107 of herbaceous annuals and perennials reaching a total vegetation height of 0.30–0.50 m (Grünzweig et al.,
108 2003, 2007). The root density range is 30–80 roots m⁻² at the upper 0.1 m soil depth, falling to the minimum
109 value (~0 roots m⁻²) at 0.7 m soil depth (Preisler et al., 2019). Biological soil crust (BSC) is evident in the
110 forest but is less than in the surrounding shrub by ~40% (Gelfand et al., 2012).

111 The soil at the research site is shallow (20–40 cm), reaching only 0.7–1.0 m; the stoniness fraction for the
112 soil depth (0–1.2 m) is 15–60%, and the rock cover of the surface ranges between 9 and 37%, as recently
113 described in detail (Preisler et al., 2019); the soil is eolian-origin loess with a clay-loam texture (31% sand,
114 41% silt, and 28% clay; density: 1.65 ± 0.14 g cm⁻³) overlying chalk and limestone bedrock. Deeper soils
115 (up to 1.5 m) are sporadically located at topographic hollows. While the natural rocky hill slopes in the
116 region are known to create flash floods, the forested plantation reduces runoff dramatically to less than 5%
117 of annual rainfall (Shachnovich et al., 2008). Groundwater is deep (>300 m), reducing the possibility of
118 groundwater recharge due to negative hydraulic conductivity or of water uptake by trees from the
119 groundwater.

120 2.2. Flux and meteorological measurements

121 An instrumented eddy covariance (EC) tower was erected in the geographical center of Yatir forest,
122 following the EUROFLUX methodology (Aubinet et al., 2000). The system uses a three-dimensional (3D)
123 sonic anemometer (Omnidirectional R3, Gill Instruments, Lymington, UK) and a closed path LI-COR
124 7000 CO₂/H₂O gas analyzer (LI-COR Inc., Lincoln, NE, USA) to measure the evapotranspiration flux (ET)
125 and net CO₂ flux (NEE). EC flux measurements were used to estimate the annual scale of NEP by

126 integrating half-hour NEE values. The long-term operation of our EC measurement site (since 2000; see
 127 Rotenberg and Yakir, 2010) provides continuous flux and meteorological data with about 80% coverage,
 128 which are subjected to U^* night-time correction and quality control, and gap filling is based on the extent
 129 of the missing data, as recently described in more detail in Tatarinov et al. (2016). A site-specific algorithm
 130 was used for flux partitioning into R_e and GPP. Daytime ecosystem respiration (R_{e-d} , in $\mu\text{mol m}^{-2} \text{s}^{-1}$) was
 131 estimated based on measured night-time values (R_{e-n} ; i.e., when the global radiation was $<5 \text{ W m}^{-2}$),
 132 averaged for the first three half-hours of each night. The daytime respiration for each half-hour was
 133 calculated according to Eq. 3 (Maseyk et al., 2008a; Tatarinov et al., 2016):

$$134 \quad R_{e-d} = R_{e-n}(\alpha_1\beta_s^{dT_s} + \alpha_2\beta_w^{dT_a} + \alpha_3\beta_f^{dT_a}) \quad (3)$$

135 where β_s , β_w , and β_f are coefficients that correspond to soil, wood, and foliage, respectively; dT_s and dT_a
 136 are soil and air temperature deviations from the values at the beginning of the night; and α_1 , α_2 , and α_3 are
 137 partitioning coefficients fixed at 0.5, 0.1, and 0.4, respectively. The β_s , β_w , and β_f coefficients were
 138 calculated as follows: β_s values were based on Q_{10} from the Grünzweig et al. (2009) study at the same site;
 139 where $\beta_s = 2.45$ for wet soil (i.e., SWC in the upper 30 cm above 20% vol); $\beta_s = 1.18$ for dry soil (i.e.,
 140 SWC in the upper 30 cm equal to or below 20% vol); $\beta_f = 3.15 - 0.036 T_a$; and $\beta_w = 1.34 + 0.46 \exp(-$
 141 $0.5((\text{DoY}-162)/66.1)^2)$, where DoY is the day of the hydrological year starting from 1 October. Finally,
 142 GPP was calculated as $\text{GPP} = \text{NEE} - R_e$. Negative values of the NEE and GPP indicated that the ecosystem
 143 was a CO_2 sink.

144 Half-hour auxiliary measurements used in this study included photosynthetic activity radiation (PAR mol
 145 $\text{m}^{-2} \text{s}^{-1}$), vapor pressure deficit (VPD, kPa), wind speed (m s^{-1}), and relative humidity (RH, %), with
 146 additional measurements as described elsewhere (Tatarinov et al., 2016). Furthermore, the soil
 147 microclimatology half-hour measurements were measured and calculated with soil chamber
 148 measurements, using the LI-8150-203 (LI-COR, Lincoln, NE), as described below, namely air temperature
 149 (T_a , $^{\circ}\text{C}$) and relative humidity (RH, %) at 20 cm above the soil surface and soil temperature (T_s , $^{\circ}\text{C}$) at a
 150 5 cm soil depth using a soil temperature probe, as well as volumetric soil water content (SWC_{0-10} , $\text{m}^3 \text{m}^{-3}$)
 151 in the upper 10 cm of the soil near the chambers, using the ThetaProbe model ML2x (Delta-T Devices
 152 Ltd., Cambridge, UK), which was calibrated to the soil composition based on the manufacturer's equations.

153 **2.3. Soil CO_2 fluxes**

154 Soil CO_2 fluxes (R_s) were measured with automated non-steady-state systems, using 20 cm diameter
 155 opaque chambers and a multiplexer to allow for simultaneous control of several chambers (LI -8150, -
 156 8100-101, -8100-104; LI-COR, Lincoln, NE). The precision of CO_2 measurements in the chambers' air is
 157 $\pm 1.5\%$ of the measurements' range (0–20,000 ppm). The chambers were closed on preinstalled PVC collars

158 20 cm diameter, allowing for short measurement time (i.e., 2 min), and positioned away from the collars
 159 for the rest of the time. Data were collected using a system in which air from the chambers was circulated
 160 (2.5 l min⁻¹) through an infrared gas analyzer (IRGA) to record CO₂ (μmol CO₂/mol air) and H₂O (mmol
 161 H₂O/mol air) concentrations in the system logger (1 s⁻¹). Gap filling of missing data due to technical
 162 problems (i.e., 27 % of the data across the study period between November 2015 and October 2016) was
 163 based on the average diurnal cycle of each month.

164 The rates of soil CO₂ flux, R_s (μmol CO₂ m⁻² s⁻¹), were calculated from chamber data using a linear fit of
 165 change in water-corrected CO₂ mole fraction using Eq. 4 (LiCor Manual, 2015) as follows:

$$166 \quad R_s = \frac{dC}{dt} \cdot \frac{vP}{sT_aR} \quad (4)$$

167 where dC/dt is the rate of change in the water-corrected CO₂ mole fraction (μmol CO₂ mol⁻¹ air s⁻¹), v is
 168 the system volume (m³), P is the chamber pressure (Pa), s is the soil surface area within the collar (m²), T_a
 169 is the chamber air temperature (K), and R is the gas constant (J mol⁻¹ K⁻¹). A measurement period of 2
 170 minutes was used, based on preliminary tests to obtain the most linear increase of CO₂ in the chambers
 171 with the highest R².

172 Soil CO₂ fluxes in the experimental plot were measured between November 2015 and October 2016 by
 173 means of three measurement chambers using 21 collars grouped in seven sites in the forest stand, with
 174 three locations (i.e., three collars) per site, based on different distances from the nearest tree (Dt). The
 175 collars were inserted 5 cm into the soil. Data were recorded on a half-hour basis (48 daily records). The
 176 three chambers were rotated between the seven sites every 1–2 weeks to cover all sites and to assess spatial
 177 and temporal variations.

178 Upscaling of the collar measurements to plot-scale soil CO₂ flux was carried out by grouping collars based
 179 on three locations (i.e., under trees [<1 m from nearest tree; UT], in gaps between trees [1–2.3 m; BT], and
 180 in open areas [>2.3 m; OA]), with one chamber taking measurements at each location, and estimating the
 181 fractional areas (Ø) of the three locations based on mapping the sites according to the distances noted
 182 above, as previously done by Raz-Yaseef et al. (2010):

$$183 \quad R_s = R_{sOA} * \varnothing_{OA} + R_{sBT} * \varnothing_{BT} + R_{sUT} * \varnothing_{UT} \quad (5)$$

$$184 \quad \varnothing_{OA} + \varnothing_{BT} + \varnothing_{UT} = 1 \quad (6)$$

185 The annual scale of R_s was derived from the upscaled chamber measurements (Eq. 5) based on daily
 186 records (48 half-hourly values) of spatial upscaled R_s.

187 Estimating the temperature sensitivity of R_s (Q₁₀) was performed as described by Davidson and Janssens
 188 (2006) using a first-order exponential equation (see also Xu et al., 2015):

189
$$R_s = a e^{bT_s} \quad (7)$$

190 where R_s represents the half-hour spatial upscaled time series of soil respiration flux ($\mu\text{mol m}^{-2} \text{s}^{-1}$), T_s
 191 ($^{\circ}\text{C}$) is soil temperature at a 5 cm depth (upscaled spatially and temporally using the same method as for
 192 R_s), and a and b are fitted parameters. The b values were used to calculate the Q_{10} value according to the
 193 following equation:

194
$$Q_{10} = e^{10b} \quad (8)$$

195 **2.4. Soil CO₂ flux partitioning**

196 Determination of different sources of soil CO₂ efflux was based on linear mixing models (Lin et al., 1999)
 197 to estimate proportions for three main sources (autotrophic, heterotrophic, and abiotic), using isotopic
 198 analysis of soil CO₂ profiles and soil incubation data from eight campaigns (January to September) during
 199 2016, according to Equations 9–11. Partitioning of the monthly R_s values into components was done using
 200 a 3-endmember triangular model for interpreting the $\delta^{13}\text{C}$ and $\Delta^{14}\text{C}$ values of CO₂ flux; the 3-endmember
 201 triangular corners are the autotrophic (R_{sa}), heterotrophic (R_h), and abiotic (R_i) sources of R_s . The $\delta^{13}\text{C}$
 202 and $\Delta^{14}\text{C}$ isotope signatures of monthly R_s locate it inside the triangle (SI Fig. 2):

203
$$\delta^{13}\text{C}_{R_s} = f_{sa} * \delta^{13}\text{C}_{sa} + f_h * \delta^{13}\text{C}_h + f_i * \delta^{13}\text{C}_i \quad (9)$$

204
$$\Delta^{14}\text{C}_{R_s} = f_{sa} * \Delta^{14}\text{C}_{sa} + f_h * \Delta^{14}\text{C}_h + f_i * \Delta^{14}\text{C}_i \quad (10)$$

205
$$1 = f_{sa} + f_h + f_i \quad (11)$$

206 where f indicates the fraction of total soil flux (e.g., $f_h=R_h/R_s$), while subscripts sa , h , and i indicate
 207 autotrophic, heterotrophic, and inorganic components, respectively. The three-equations system was used
 208 to solve the three unknown f fractions of the total soil flux based on empirical estimates of the isotopic
 209 endmembers. Additionally, $\delta^{13}\text{C}$ and $\Delta^{14}\text{C}$ are the stable and radioactive carbon isotopic ratios, where $\delta^{13}\text{C}$
 210 = $[(^{13}\text{C}/^{12}\text{C})_{\text{sample}}/(^{13}\text{C}/^{12}\text{C})_{\text{reference}}]-1]*1000\text{‰}$ and the reference is the Vienna international standard
 211 (VPDB). Radiocarbon data are expressed as $\Delta^{14}\text{C}$ in parts per thousand or per mil (‰), which is the
 212 deviation of a sample $^{14}\text{C}/^{12}\text{C}$ ratio relative to the OxI standard in 1950 (see Taylor et al., 2015), that is,
 213 $\Delta^{14}\text{C} = [(^{14}\text{C}/^{12}\text{C})_{\text{sample}}/(0.95*[^{14}\text{C}/^{12}\text{C}]_{\text{reference}}*\exp[(y-1950)/8267])]-1]*1000\text{‰}$, where y is the year of
 214 sample measurements.

215 The $\delta^{13}\text{C}_{R_s}$ was estimated monthly using the Keeling plot approach (SI Figs 3 and 4; Pataki et al., 2003;
 216 Taneva and Gonzalez-Meler, 2011). Soil air was sampled using closed-end stainless steel tubes (6 mm
 217 diameter) perforated near the tube bottom at four depths (30, 60, 90, and 120 cm). Samples of soil air were
 218 collected in pre-evacuated 150 mL glass flasks with high-vacuum valves, the dead volume in the tubing
 219 and flask necks having been purged with soil air using a plastic syringe equipped with a three-way valve.

220 Note that the Keeling plot approach is based on the 2-endmembers mixing model (see Review of Pataki et
221 al., 2003), which often does not hold in soils because of variations in the $\delta^{13}\text{C}$ values of source material
222 with depth (see a recent example in Joseph et al., 2019). However, probably because of the very dry
223 conditions at our study site, no change in $\delta^{13}\text{C}$ with depth in the root zone is observed ($\pm 0.1\%$ across the
224 35 cm depth profiles; SI Fig. 5), providing an opportunity to avoid this caveat, we must also conclude of
225 course that the variations among the contributions of Rsa, Rh, and Ri do not change significantly with
226 depth and permitting the use of the single set of isotopic signatures in Table 2. The soil CO_2 samplings
227 carried out therefore represented predominantly the mixing of atmospheric CO_2 with a single integrated
228 soil source signal, consistent with the Keeling plot approach.

229 The autotrophic ($\delta^{13}\text{C}_{\text{sa}}$) endmember was estimated based on incubations during the sampling periods of
230 excised roots, following Carbone et al. (2008). Fine roots (<2 mm diameter) were collected, rinsed with
231 deionized water, and incubated for 3 hours in 10 mL glass flasks connected with Swagelok Ultra-Torr tee
232 fittings to 330 mL glass flasks equipped with Louwers high-vacuum-valves. The flasks were flushed with
233 CO_2 -free air at room temperature close to field conditions. The CO_2 was allowed to accumulate to at least
234 2,000 ppm (~2 h).

235 The heterotrophic ($\delta^{13}\text{C}_{\text{h}}$) endmember was estimated as in Taylor et al. (2015), and, similar to the root-
236 incubation experiment, soil samples from the top 5 cm of the litter layer or 10 cm below the soil surface
237 were collected, and roots were carefully removed to isolate heterotrophic components. Root-free soils were
238 placed in 10 mL glass flasks and allowed to incubate for 24 hours before being transferred to evacuated
239 330 mL glass flasks. The inorganic source ($\delta^{13}\text{C}_{\text{i}}$) endmember was estimated using one gram of dry soil
240 (ground to pass through a 0.5 mm mesh) placed in a 10 mL tube with a septum cap; then, 12 mL of 1M
241 HCl was added to dissolve the carbonate fraction, and the fumigated CO_2 withdrawn from each tube was
242 collected using a 10 mL syringe and injected into a 330 mL evacuated flask for isotopic analysis.

243 Radiocarbon estimates were based on the work of Carmi et al. (2013) at the same site, adjusted to the
244 measured atmospheric ^{14}C values during the study period (49.5‰; Carmi et al., 2013). The $\Delta^{14}\text{C}_{\text{sa}}$ and
245 $\Delta^{14}\text{C}_{\text{h}}$ endmembers were estimated based on the assumption that they carry the ^{14}C signatures of 4 and 8.5
246 years, respectively, older than the ^{14}C signature of the atmosphere at the time of sampling, based on mean
247 ages previously estimated (Graven et al., 2012; Levin et al., 2010; Taylor et al., 2015). $\Delta^{14}\text{C}_{\text{i}}$ was obtained
248 from Carmi et al. (2013). Monthly values of $\Delta^{14}\text{C}_{\text{Rs}}$ were obtained using the linear equation of the
249 regression line of the measured $\delta^{13}\text{C}$ values of Rsa, Rsh, and Ri and the corresponding estimated $\Delta^{14}\text{C}$
250 values (SI Fig. 2) and monthly $\delta^{13}\text{C}$ values of Rs.

251 **2.5. Isotopic analysis**

252 Isotopic analysis followed the methodology described in Hemming et al. (2005). The $\delta^{13}\text{C}$ of CO_2 in the
253 air was analyzed using a continuous flow mass spectrometer connected to a 15-flask automatic manifold
254 system. An aliquot of 1.5 mL of air was expanded from each flask into a sampling loop on a 15-position
255 valve (Valco Houston, TX, USA). CO_2 was cryogenically trapped from the air samples using helium as a
256 carrier gas; it was then separated from N_2O with a Carbosieve G (Sigma Aldrich) packed column at 70°C
257 and analyzed on a Europa 20-20 Isotope Ratio Mass Spectrometer (Crewe, UK). $\delta^{13}\text{C}$ results were quoted
258 in parts per thousand (‰) relative to the VPDB international standard. The analytical precision was 0.1‰.
259 To measure $[\text{CO}_2]$, an additional 40.0 mL subsample of air from each flask was expanded into mechanical
260 bellows and then passed through an infrared gas analyzer (LICOR 6262; Lincoln, NE, USA) in an
261 automated system. The precision of these measurements was 0.1 ppm. Flasks filled with calibrated standard
262 air were measured with each batch of 10 sample flasks; five standards were measured per 10 samples for
263 $\delta^{13}\text{C}$ analyses and four standards per 10 samples for $[\text{CO}_2]$ analyses.

264 Organic matter samples were dried at 60°C and milled using a Wiley Mill fitted with size 40 mesh, and
265 soil samples were ground in a pestle and mortar. Soils containing carbonates were treated with 1M
266 hydrochloric acid. Between 0.2 and 0.4 mg of each dry sample was weighed into tin capsules (Elemental
267 Microanalysis Ltd., Okehampton, UK), and the $\delta^{13}\text{C}$ of each was determined using an elemental analyzer
268 linked to a Micromass Optima IRMS (Manchester, UK). Three replicates of each sample were analyzed,
269 and two samples of a laboratory working standard cellulose were measured for every 12 samples. Four
270 samples of the acetanilide (Elemental Microanalysis Ltd.) international standard were used to calibrate
271 each run, and a correction was applied to account for the influence of a blank cup. The precision was 0.1‰.

272 **2.6. Total belowground carbon allocation (TBCA)**

273 TBCA ($\text{g C m}^{-2} \text{y}^{-1}$) was calculated following Giardina and Ryan (2002) for the study year (November
274 2015–October 2016) as follows:

$$275 \quad \text{TBCA} = R_s - R_{\text{alp}} + \Delta C_{\text{soil}} \quad (12)$$

276 where R_{alp} is the annual aboveground litter production between November 2014 and October 2015, and
277 ΔC_{soil} is the annual change in belowground total soil organic C. Litter production, not measured during the
278 present study, was estimated based on values obtained by Masyk et al. (2008b) for 2000–2006 (56 g C m^{-2}
279 y^{-1}) and assumed to have increased in the study period (2014–2015) proportionally to the measured
280 increase in leaf area index (LAI; 1.31 to 1.94; i.e., $R_{\text{alp}} = [(1.94*56)/1.31] = 83 \text{ g C m}^{-2} \text{y}^{-1}$). For herbaceous
281 litter production, three plots of 25 m^2 were randomly selected in 2002 and harvested at the end of the
282 growing season, total fresh biomass was weighed, and subsamples were used to determine dry weight and
283 C content. Grünzweig et al. (2007) found that herbaceous litter production was close to the average rainfall

284 for the specific year; this method was adapted in the current study for the period between November 2014
285 and October 2015. Since aboveground litter (R_{alp} ; the sum of tree litter and herbaceous litter production)
286 of a given year was mainly produced during that year but decayed during the following hydrological year,
287 TBCA was on the current year's R_s (2015–2016) and the previous year's R_{alp} (2014–2015). ΔC_{soil} was set
288 constant as the average annual belowground carbon increase since afforestation (Qubaja et al., in press).

289 **2.6. Statistical analyses**

290 Two-way ANOVA tests were performed at a significance level set at $p = 0.001$ to detect significant effects
291 of locations (OA, BT, and UT), sites, and their interactions on R_s and meteorological parameters. Pearson
292 correlation analysis (r) was used to detect the correlation between R_s and meteorological parameters. To
293 quantify spatio-temporal variability in R_s , the coefficient of variation (CV%) was calculated as
294 $[(STDEV/Mean)*100\%]$. Heterogeneity was considered weak if $CV\% \leq 10\%$, moderate if $10\% < CV\% \leq$
295 100% , and strong if $CV\% > 100\%$. All the analyses were performed using Matlab software, Version
296 R2017b (MathWorks, Inc., MA, USA).

297 **3. Results**

298 **3.1. Spatial variations**

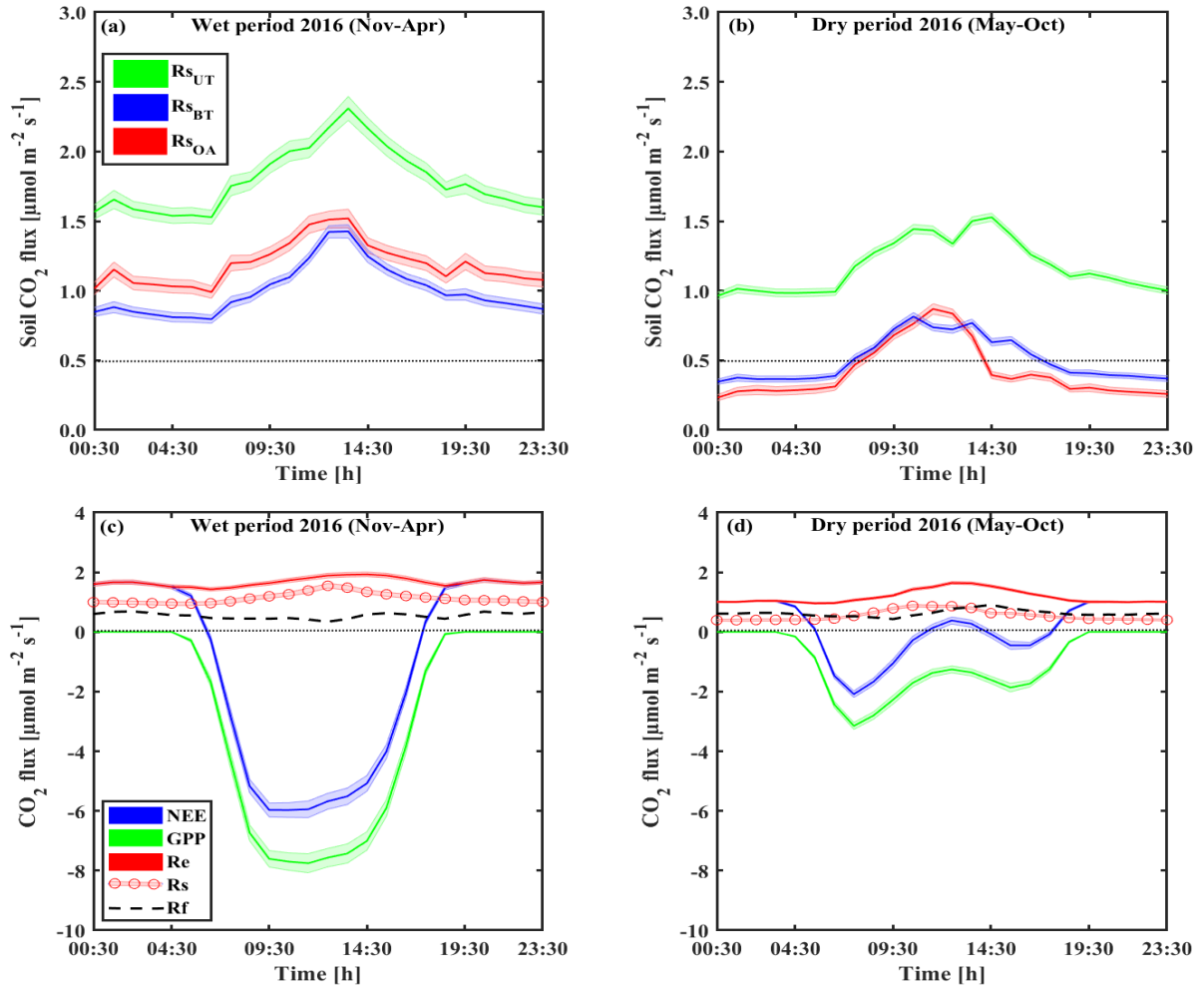
299 The spatial variations in R_s across locations (distance from nearest tree) and sites (across the study area)
300 are reported in Table 1, together with other measured variables. The results indicated an overall mean R_s
301 value of $0.8 \pm 0.1 \mu\text{mol m}^{-2} \text{s}^{-1}$, with distinct values for the three locations. R_s was greater at UT locations
302 than at the BT and OA locations by a factor of ~ 2 . The spatial variability among the locations was also
303 apparent in the R_s daily cycle (Fig. 1), with clear differences between the wet season (November to April),
304 when the UT showed consistently higher R_s values than at other locations by a factor of about 1.6 and the
305 dry season by a factor of approximately 2.6. Note that the daily peak in R_s remained at midday in both the
306 wet and dry seasons. Overall, the 21 collars showed moderate variations ($CV = 55\%$; Table 1), R_s was
307 negatively correlated with distance from trees (D_t ; $r = -0.62$; $p < 0.01$) and with soil and air temperatures
308 (T_s and T_a ; $r = -0.45$; $p < 0.05$), and positively correlated with soil water content and relative humidity
309 (SWC and RH; $r = 0.50$; $p < 0.05$). The inverse correlation between R_s and distance from the nearest tree
310 could be useful in considering the expected decline in stand density due to thinning and mortality (e.g.,
311 associated with a drying climate). For a first approximation, the results indicate that decreasing from the
312 present stand density of 300 trees ha^{-1} to 100 trees ha^{-1} and the resulting increase in mean distance among
313 trees could result in decreasing ecosystem R_s by 11%.

314 **Table 1** Annual mean of half-hour values across locations (OA, open area; BT, between trees; UT, under tree) in
 315 seven sites in the forest during the study period, of soil respiration flux rates (Rs) together with the soil water content
 316 at 10 cm depth (SWC), minimum distances from nearby tree (Dt), soil temperature at 5 cm depth (Ts), and air
 317 temperature (Ta) and relative humidity (RH) at the soil surface (numbers in parenthesis indicate \pm se).

Locations	Sites	Rs [$\mu\text{mol m}^{-2} \text{s}^{-1}$]	SWC [x100 $\text{m}^3 \text{m}^{-3}$]	Dt [m]	Ts [$^{\circ}\text{C}$]	Ta [$^{\circ}\text{C}$]	RH [%]
OA	1	1.64 (0.02)	16.5 (0.2)	2.9	15.6 (0.1)	15.4 (0.2)	59.7 (0.5)
	2	0.72 (0.01)	14.5 (0.2)	3.6	15.9 (0.2)	15.0 (0.2)	58.4 (0.6)
	3	1.23 (0.02)	19.3 (0.2)	7.0	20.6 (0.3)	18.2 (0.2)	53.5 (0.5)
	4	0.38 (0.01)	11.3 (0.2)	3.0	22.6 (0.2)	20.8 (0.1)	58.9 (0.4)
	5	0.38 (0.01)	5.8 (0.2)	3.0	25.5 (0.1)	24.0 (0.1)	43.1 (0.4)
	6	0.31 (0.01)	5.7 (0.4)	2.8	30.0 (0.3)	26.2 (0.3)	51.8 (0.9)
	7	0.14 (0.01)	6.1 (0.3)	3.5	25.5 (0.2)	23.2 (0.3)	44.5 (0.9)
	Average CV [%]	0.68 (0.21) 81 %	11 (0) 50%	3.7 (0.6) 41%	22.3 (2.0)	20.4 (1.6)	52.8 (2.6) 13 %
BT	1	0.77 (0.01)	10.5 (0.2)	1.8	16.1 (0.1)	15.2 (0.2)	60.5 (0.5)
	2	0.88 (0.01)	12.1 (0.2)	1.5	14.8 (0.2)	14.7 (0.2)	59.5 (0.6)
	3	0.84 (0.01)	20.4 (0.2)	2.7	20.1 (0.3)	18.4 (0.2)	54.1 (0.6)
	4	0.91 (0.01)	14.4 (0.2)	2.7	23.3 (0.2)	21.3 (0.2)	58.5 (0.4)
	5	0.41 (0.00)	3.9 (0.2)	2.0	24.6 (0.1)	24.0 (0.1)	43.2 (0.4)
	6	0.41 (0.01)	3.3 (0.4)	2.5	29.1 (0.2)	26.0 (0.3)	52.5 (0.8)
	7	0.46 (0.01)	5.5 (0.3)	1.2	23.9 (0.1)	22.8 (0.3)	45.7 (0.9)
	Average CV [%]	0.67 (0.09) 35 %	10 (0) 63%	2.0 (0.2) 29%	21.7 (1.9)	20.3 (1.6)	53.4 (2.6) 13 %
UT	1	1.22 (0.02)	9.3 (0.2)	0.2	15.7 (0.1)	15.2 (0.2)	60.0 (0.5)
	2	1.42 (0.01)	14.0 (0.2)	0.3	14.8 (0.2)	14.8 (0.2)	59.4 (0.6)
	3	1.64 (0.01)	19.8 (0.2)	0.5	19.0 (0.2)	18.0 (0.2)	54.5 (0.6)
	4	1.90 (0.02)	11.3 (0.2)	0.6	22.0 (0.1)	20.8 (0.1)	59.0 (0.4)
	5	1.16 (0.01)	4.0 (0.2)	0.4	23.9 (0.1)	23.7 (0.1)	44.1 (0.4)
	6	1.29 (0.01)	4.5 (0.4)	0.2	29.5 (0.3)	25.9 (0.3)	52.7 (0.9)
	7	0.89 (0.01)	5.2 (0.3)	0.2	25.0 (0.1)	23.0 (0.3)	45.5 (0.9)
	Average CV [%]	1.36 (0.13) 25 %	10 (0) 60%	0.3 (0.1) 46%	21.4 (2.0)	20.2 (1.6)	53.6 (2.5) 12 %
All	Average (SE)	0.8 (0.1)	11 (0)	2.0 (0.4)	21.8 (1.1)	20.3 (0.9)	53.3 (1.4)
	Max	1.90	20	7.0	30.0	26.2	60.5
	Min	0.14	3	0.2	14.8	14.7	43.1
	CV [%]	55 %	55%	82%			12 %
Two-way ANOVA (P value)	Site	0.000	0.000		0.000	0.000	0.000
	Location	0.000	0.000		0.000	0.220	0.074
	Site x Location	0.000	0.000		0.000	0.645	0.961
Pearson Correlation with Rs			.50*	-.62**	-.45*	-.45*	.50*

318 ** . Correlation is significant at the 0.01 level (two-tailed).

319 * . Correlation is significant at the 0.05 level (two-tailed).



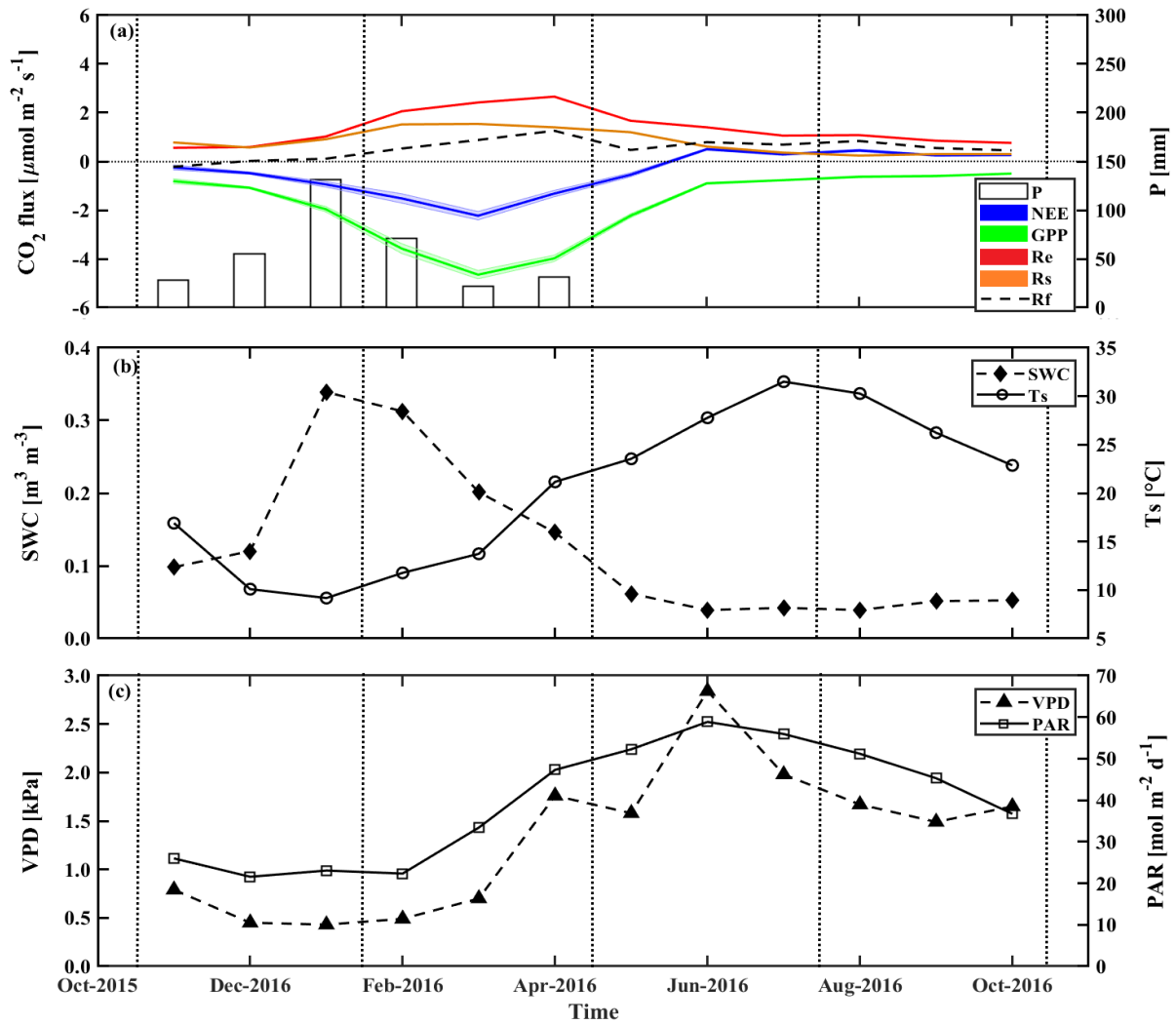
320
 321 **Figure 1** Representative diurnal cycles of soil respiration (Rs; using soil chambers across locations: open area, OA;
 322 between trees, BT; under trees, UT) and sites in panels a and b, of net ecosystem exchange (NEE; canopy scale eddy
 323 covariance) and gross primary production (GPP), and ecosystem respiration (Re) and its partitioning to soil respiration
 324 (Rs) and aboveground tree respiration (Rf) in panels c and d, during the wet (Nov–Apr) and dry (May–Oct) periods.
 325 Based on half-hour values over the diurnal cycle; shaded areas indicate $\pm se$; Rf was estimated as the residual as $R_f =$
 326 $Re - R_s$ and was presented as a dashed line.

327 3.2. Temporal dynamics

328 On the diurnal timescale, CO₂ fluxes showed typical daily cycles (Fig. 1). As expected, on average, all CO₂
 329 fluxes were higher during the wet period compared to the dry season by a factor of ~2. However, Rs and
 330 Re peaked around midday in both the wet and dry seasons, while the more physiologically controlled NEE
 331 and GPP showed a shift from midday (around 11:00–14:00) to early morning (08:00–11:00) in the dry
 332 season, with a midday depression and a secondary afternoon peak (Fig. 1d).

333 The temporal variations across the seasonal cycle are reported in Fig. 2, based on monthly mean values,
 334 exhibiting sharp differences between the wet and dry seasons. As previously observed in this semi-arid
 335 site, all CO₂ fluxes peak in early spring between March and April. The corresponding high-resolution data

336 are reported in SI Fig. 6, which show also that the high winter (February) Rs rates were associated with
 337 clear days when photosynthetic active radiation (PAR) increased with air temperature, Ta. These data also
 338 show that, following rainy days, daily Rs values could reach $6.1 \mu\text{mol m}^{-2} \text{s}^{-1}$ (i.e., in the UT microsite;
 339 data not shown), although the average was $1.1 \pm 0.2 \mu\text{mol m}^{-2} \text{s}^{-1}$ during the wet period, which diminished
 340 by $\sim 55\%$ in the dry season to mean daily values of $0.5 \pm 0.1 \mu\text{mol m}^{-2} \text{s}^{-1}$. In spring (April), all CO₂ fluxes
 341 peaked during the crossover trends of decreasing soil moisture content and increasing both temperature
 342 and PAR (SI Fig. 6).



343
 344 **Figure 2** Seasonal trends of monthly mean values during the research period of a) the fluxes of net ecosystem
 345 exchange (NEE), gross primary production (GPP), and ecosystem respiration (Re) and its components, soil respiration
 346 (Rs) and aboveground tree respiration (Rf); and monthly mean of key environmental parameters, b) soil water content
 347 at the top 10 cm (SWC₀₋₁₀) and soil temperature at 5 cm (Ts), and c) vapor pressure deficit (VPD) and photosynthetic
 348 activity radiation (PAR). Rf is obtained from the Re-Rs. Vertical dotted lines indicate the winter, spring, summer and
 349 autumn seasons.

350 The temporal variations in the half-hour values of Rs reflected changes in soil moisture at 0–5 cm depth
 351 and PAR ($r = 0.5$ and 0.2 , respectively; $p < 0.01$) and negative correlations with Ts and RH ($r = 0.2$ and

0.1, respectively; $p < 0.01$). The variations in the integrated Rs showed a CV of 71%, with the temporal variations dominated strongly by PAR (CV > 100%), moderately by SWC (CV~85%), and weakly by RH (CV~40%)(correlations and CV values were not included in figures and tables). Repeating the models applied by Grünzweig et al. (2009), the potential climatic factors that best predicted daily Rs shifted from SWC and PAR in the dry season to Ts and PAR in the wet season (SI Table 2). These equations explained 43% and 70% of the variation in Rs in the dry and wet seasons, respectively (SI Table 2). A reasonable forecast of the temporal variations in Rs ($\mu\text{mol m}^{-2} \text{s}^{-1}$) at half-hour values ($R^2 = 0.60$, $p < 0.0001$) was obtained based on SWC_{0-10} and Ts values across the entire seasonal cycle, based on:

$$\text{Rs} = 0.05126 * \exp(0.04274 * \text{Ts} + 28.51 * \text{SWC} - 74.44 * \text{SWC}^2) \quad (13)$$

At the ecosystem scale, Re was characterized by high fluxes in the wet season and peak values of $\sim 2.4 \mu\text{mol m}^{-2} \text{s}^{-1}$ in February to April (Fig. 2; SI Table 1). Re fluxes rapidly decreased after the cessation of rain and reached the lowest values in the fall (September to October), with mean dry period values of $0.5 \pm 0.1 \mu\text{mol m}^{-2} \text{s}^{-1}$ (Fig. 2, SI Table 1). GPP had a mean value of $-1.8 \pm 0.4 \mu\text{mol m}^{-2} \text{s}^{-1}$, and daily NEE had a mean value of $-0.5 \pm 0.3 \mu\text{mol m}^{-2} \text{s}^{-1}$ (SI Table 1 and SI Fig. 6), with the same seasonality (Fig. 2).

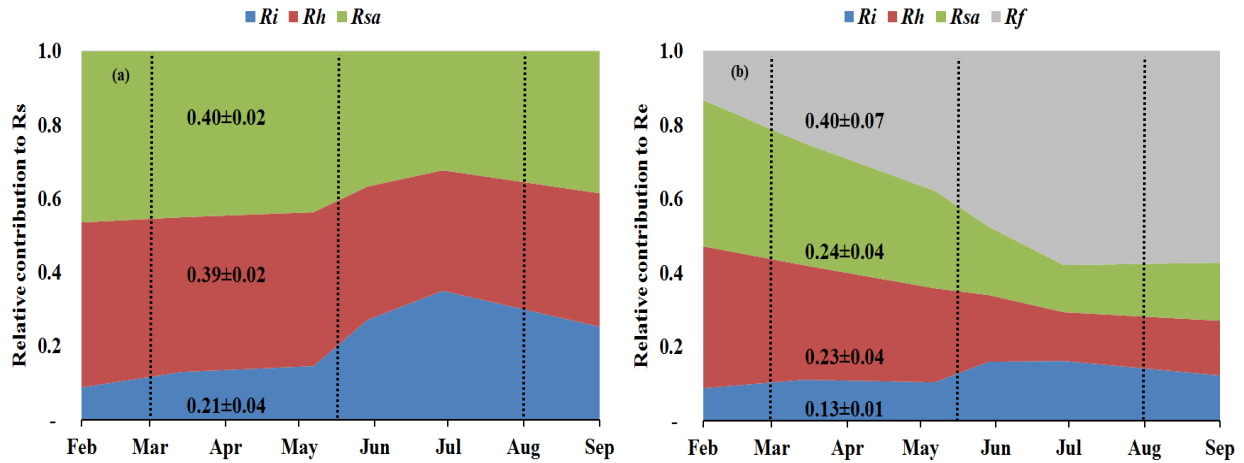
Table 2 $\delta^{13}\text{C}$ and $\Delta^{14}\text{C}$ signature of soil respiration (Rs) and its partitioning to autotrophic (Rsa), heterotrophic (Rh), and abiotic (Ri), together with the relative contribution of each to the soil and ecosystem respiration for Yatir forest during eight campaigns of measurements from January to September 2016 (numbers in parenthesis indicate \pm se) in comparison to results obtained previously in the same forest (2001–2006 mean values). The monthly contribution of Rsa, Rh, and Ri to Rs or Re is presented in Fig. 3a and b, respectively.

Signature	Rsa	Rh	Ri	Rs
	[‰]			
$\delta^{13}\text{C}$	-23.7 (0.5) ¹	-24.3 (0.0) ¹	-6.5 (0.0) ¹	-20.8 (± 0.6) ¹
$\Delta^{14}\text{C}$	30 ³	50 ³	-900 ²	-134 (34) ⁴
Relative contribution to Rs (2015–2016)	0.40 (0.02)	0.39 (0.02)	0.21 (0.04)	
Relative contribution to Re (2015–2016)	0.24 (0.04)	0.23 (0.04)	0.13 (0.01)	0.60 (0.06)

¹ Measured in the present study; ² measured by Carmi et al., (2013); ³ calculated based on the measured atmospheric value by Carmi et al. (2013); and ⁴ calculated based on the best fit regression equation in SI Fig. 2.

Figure 3 (see also Table 2) summarizes the seasonal variations in Rs and Re partitioning. The monthly Rsa and Rh were not significantly different but were significantly different from Ri ($p < 0.05$). The Rsa/Rs ratios ranged from 0.32 to 0.46, the largest contribution occurring in early spring from February to April. The Rh/Rs fraction ranged between 0.33 and 0.45, being the highest during the wet season. The Ri/Rs – the fraction of inorganic sources from the total soil respiration – ranged from 0.09 to 0.35, the largest contribution being in the driest period. The mean relative contributions of these components to Rs over the sampling campaigns are presented in Figure 3a, but, on average, soil biotic fluxes were higher than abiotic fluxes by a factor of ~ 4 . Re partitioning showed an average increase in Rf/Re from 25% in the wet season to 54% in the dry season and a decline in Rs/Re from 75% to 46% on average in the wet and the dry seasons, respectively, which reflected a seasonal change of Rf in the wet season to peak values in the dry

383 season (Fig. 3b). Both the highest and lowest Rs fractions (~0.74 and nearly 0.34) along the seasonal cycle
 384 were associated with low total Re fluxes, that is, in the fall before the Rf peak in the spring and in the
 385 summer, when physiological controls limited water loss (Fig. 2).



386
 387 **Figure 3.** a) Seasonal variations in the relative contribution of soil autotrophic (Rsa), heterotrophic (Rh), and abiotic (Ri) components to Rs, and b) seasonal variations in the relative contribution of soil autotrophic (Rsa), heterotrophic (Rh), abiotic (Ri), and foliage and stem respiration (Rf) is obtained from the Re-Rs) components to ecosystem
 388 respiration (Re) during eight campaigns (Jan–Sep) in 2016. The contributions were estimated with linear mixing
 389 models using $\delta^{13}\text{C}$ and $\Delta^{14}\text{C}$ of soil respiration (Rs) and of soil CO_2 profile method at 0 to 120 cm soil depth. Vertical
 390 dotted lines indicate the winter, spring, summer and autumn seasons. These results confirmed earlier estimates of
 391 Grünzweig et al. (2009) and Maseyk et al. (2008a).
 392
 393

394 3.3. Annual scale

395 **Table 3** Mean annual values of ecosystem respiration (Re), its components and associated ratios, net ecosystem
 396 exchange (NEE; from eddy covariance), net primary productivity (NPP), gross primary productivity (GPP), carbon-
 397 use efficiency (CUE), leaf area index (LAI), and ratio of total belowground carbon allocation (TBCA) to GPP
 398 (TBCA/GPP) in the present study (mean of Nov 2015 to Oct 2016) and in comparison to results obtained previously
 399 in the same forest (2001–2006 mean values). Ri, Rh, Rsa, Rs, Rl and Rw denote abiotic, heterotrophic, soil
 400 autotrophic, soil, foliage, and wood CO_2 flux, respectively. Q_{10} is derived during the two studies for the wet and dry
 401 season.

Study	Rs	Rh	Rsa	Rl	Rw	Ri	Re	NEE	NPP	GPP
	[g m ⁻² y ⁻¹]									
Mean (2001–2006)	406	147	203	260	70	56	735	-211	-358	-880
x/Rs		0.36	0.50			0.14				
x/Re	0.55	0.20	0.28	0.35	0.10	0.07				
Mean (2015–2016)	295	115	119	155	39	61	488	-167	-282	-655
x/Rs		0.39	0.40			0.21				
x/Re	0.60	0.23	0.24	0.32	0.08	0.13				
Ratio of (x/Rs) ₂₀₁₆ /(x/Rs) ₂₀₀₃		1.08	0.81			1.50				
Ratio of (x/Re) ₂₀₁₆ /(x/Re) ₂₀₀₃	1.09	1.18	0.88	0.90	0.84	1.64				
Study	Q ₁₀		CUE	TBCA/GPP ³	LAI					
	SWC ¹	SWC ²			[m ² m ⁻²]					
Mean (2001–2006)	2.5	1.2	0.40	0.41	1.3					
Mean (2015–2016)	1.6	1.1	0.43	0.38	2.1					
Ratio of x ₂₀₁₆ /x ₂₀₀₃	0.64	0.92	1.06	0.93	1.62					

403 ¹ SWC ≥ 0.2 [$\text{m}^3 \text{m}^{-3}$] and ² SWC < 0.2 [$\text{m}^3 \text{m}^{-3}$]; ³ and the mean of GPP used by Grünzweig et al., 2009 to estimate
404 the TBCA/GPP was $834 \text{ g C m}^{-2} \text{ y}^{-1}$.

405 On an annual timescale, estimates of CO₂ flux components based on EC measurements resulted in annual
406 values of GPP, NPP, Re, and NEP of 655, 282, 488, and 167 $\text{g C m}^{-2} \text{ y}^{-1}$, respectively (Tables 3 and SI-1).
407 On average across the measurement period, Rs was the main CO₂ flux to atmosphere, making up $60 \pm 6\%$
408 of Re ($295 \pm 4 \text{ g C m}^{-2} \text{ y}^{-1}$; Tables 3 and SI-1), and Rf was another significant component accounting for
409 $40 \pm 6\%$ of Re (Fig. 3b), which reflected the low density ($300 \text{ trees ha}^{-1}$) nature of the semi-arid forest. As
410 indicated above, Re partitioning showed a decrease in Rs/Re and an increase in Rf/Re from winter to
411 summer, which is clearly apparent in Fig. 3b. On an annual scale, during the study period, estimates of Rf,
412 Rsa, Rh, and Ri values were 194 ± 36 , 119 ± 21 , 115 ± 20 , and $61 \pm 6 \text{ g C m}^{-2} \text{ y}^{-1}$, respectively. These rates
413 of respiration fluxes translated at the ecosystem scale to Re/GPP of $\sim 75\%$, lower than observed in other
414 ecosystems (SI Table 3) and leading, in turn, to high ecosystem CUE of 0.43.

415 Using the site records of nearly 20 years, long-term trends in GPP, NPP, Re, and NEP were examined. Soil
416 respiration and its partitioning could not be similarly monitored continuously, but combining the present
417 results with the 2001–2006 values obtained by Grünzweig et al. (2009) and Maseyk et al. (2008a) provided
418 a basis for estimating the long-term trends in soil respiration. Notably, no clear or significant trend over
419 time was observed in any of the canopy-scale continuously monitored fluxes, but, because of relatively
420 large interannual variations, associated mainly with those in precipitation (see Qubaja et al., in press), it is
421 likely that the relative contributions of the different fluxes, expressed as ratios in Table 3, provide a more
422 robust perspective of the long-term temporal changes in the ecosystem functioning. The results presented
423 in Table 3 reflect the long-term growth of the forest, with a relatively large increase in LAI, but the TBCA
424 remained around 40%. The results also indicated little change in the total soil respiration, Rs, component,
425 (as a fraction of Re or GPP), but a general shift from the autotrophic components to the heterotrophic
426 component (i.e., Rh). This was reflected in the decreasing ratio of the autotrophic components (i.e., Rsa,
427 Rl, and Rw) to Re, and the increasing ratio of Rh (Table 3) across the 13-year observation period (2003 to
428 2016).

429 **4. Discussion**

430 Partitioning ecosystem carbon fluxes and long-term observational studies are key to understanding
431 ecosystem carbon dynamics and their response to change. Overall, the results support our research
432 hypothesis that the observed high CUE at our site is at least partly due to the characteristics of the carbon
433 flux partitioning that can be associated with the semi-arid conditions. Compared to other sites and climates
434 (see comparative compilation in SI Table 3), the results reflect several key points: 1) relatively high
435 belowground allocation; 2) low soil respiration in general, and low heterotrophic respiration in particular;

436 3) combining the results for 2016 and those of our earlier study offered a long-term perspective across 13
437 years, indicating that the low R_s in this ecosystem is robust and exhibits reduced sensitivity to temperature,
438 and 4) there is a general long-term shift from autotrophic to heterotrophic respiration.

439 Comparing CO_2 fluxes in this forest with fluxes in a range of European forests showed that mean NEP in
440 the semi-arid forest ($167 \text{ g C m}^{-2} \text{ y}^{-1}$) is similar to the mean NEP in other European forests ($150 \text{ g C m}^{-2} \text{ y}^{-1}$;
441 FLUXNET).

442 Carbon partitioning belowground (TBCA/GPP) was relatively high ($\sim 38\%$), with little change across the
443 long-term observation period. It is, however, within the range of mean value for forests in different biomes
444 (Litton et al., 2007). High belowground allocation helps explain the high rate of SOC accumulation
445 observed over the period since afforestation (Grünzweig et al., 2007; Qubaja et al., in press). Note that,
446 irrespective of the soil carbon accumulation, the abiotic component to the CO_2 flux seems to be significant
447 in dry environments (Table 3) and in particular in the dry seasons, when biological activities drastically
448 decrease (Kowalski et al., 2008; Lopez-Ballesteros et al., 2017; Serrano-Ortiz et al., 2010; Martí-Roura et
449 al., 2019). The results show that considering the abiotic effects on estimating soil respiration and, in turn,
450 on estimating the carbon budget in dry calcareous soils can play an important part in estimating soil and
451 ecosystem respiration fluxes (Angert et al., 2015; Roland et al., 2012).

452 The soil CO_2 efflux in the semi-arid forest ($295 \text{ g C m}^{-2} \text{ y}^{-1}$) is at the low end of R_s values across the range
453 of climatic regions, from 50 to $2,750 \text{ g C m}^{-2} \text{ y}^{-1}$ (Adachi et al., 2017; Chen et al., 2014; Grünzweig et al.,
454 2009; Hashimoto et al., 2015). This is clearly lower than the mean R_s value for global evergreen needle
455 forests, which is estimated at $690 \text{ g C m}^{-2} \text{ y}^{-1}$ (Chen et al., 2014), and between estimates for desert scrub
456 and Mediterranean woodland ($224\text{--}713 \text{ g C m}^{-2} \text{ y}^{-1}$; Raich and Schlesinger, 1992) or for Mediterranean
457 forests ($561\text{--}1,015 \text{ g C m}^{-2} \text{ y}^{-1}$; Casals et al., 2011; Luysaert et al., 2007; Matteucci et al., 2015; Misson et
458 al., 2010; Rey et al., 2002; Rodeghiero and Cescatti, 2005). The mean instantaneous rate of R_s , $0.8 \mu\text{mol}$
459 $\text{m}^{-2} \text{ s}^{-1}$, is also in the range reported for unmanaged forest and grassland in the dry Mediterranean region
460 (0.5 and $2.1 \mu\text{mol m}^{-2} \text{ s}^{-1}$; Correia et al., 2012).

461 The observed low R_s values were associated with a relatively high fraction of autotrophic and a lower
462 fraction of heterotrophic respiration. The mean annual-scale R_{sa}/R_s ratio of 0.40 was at the high end of the
463 global range of 0.09 to 0.49 (Chen et al., 2014; Hashimoto et al., 2015). In contrast, heterotrophic
464 respiration showed an annual-scale R_h/R_s ratio of 0.39 ± 0.02 (Table 2 and Fig. 3), which is lower than the
465 estimated global mean R_h/R_s value of 0.56 (Hashimoto et al., 2015), but within the range of Mediterranean
466 region forest, which varies between 0.29 to 0.77 (Casals et al., 2011; Luysaert et al., 2007; Matteucci et
467 al., 2015; Misson et al., 2010; Rey et al., 2002; Rodeghiero and Cescatti, 2005). The relatively low annual

468 scale of the heterotrophic respiration to R_s is consistent with the dry soil over much of the year in this
469 forest (Fig 2 and SI Fig. 6) and the observed low decomposability of plant detritus and high mean SOC
470 accumulation rate (Grünzweig et al., 2007).

471 The long-term perspective from the 13-year observation period indicates emerging trends that can be a
472 basis for assessing the effects of forest age and the evident increase in LAI (Table 3) and changes in
473 environmental conditions (generally warming and drying; see, e.g., Lelieveld et al., 2012). Here, because
474 comparing the non-continuous data from the present (2016) and earlier (2001–2006) studies is sensitive to
475 the large interannual variations in the ecosystem activities and fluxes (Qubaja et al., in press), we focused
476 on the more robust changes in the ratio of the respiration components to the overall fluxes (R_e) (Table 3).
477 This shows a shifting trend from the autotrophic components to the heterotrophic, with little change in the
478 contribution of R_s to the overall efflux. The ratios of R_{sa} , R_l , and R_w to R_e tended to decrease by about
479 13%, while that of R_h increased by about 18%; similar trends were seen in soil respiration, with R_{sa}/R_s
480 decreasing by -19% and R_h/R_s increasing by +8% (Table 3). The relatively low R_s under conditions of
481 high temperature in the semi-arid ecosystem implies reduced sensitivity of respiration to temperature. This
482 is partly imposed by low SWC conditions during extended parts of the year (Grünzweig et al., 2009; cf.
483 Rey et al., 2002; Xu and Qi, 2001). Accordingly, R_s showed greater sensitivity to T_s in the wet period, but
484 during the 8–9 months of the year when SWC was below $\sim 0.2 \text{ m}^3 \text{ m}^{-3}$, R_s varied predominantly with water
485 availability. The long-term perspective reported in Table 3 indicates a further decrease in temperature
486 sensitivity, with mean Q_{10} values in the dry season decreasing from 1.6 to 1.1. These estimated Q_{10} values
487 are generally consistent with published values for different ecosystems (1.4 to 2.0; Hashimoto et al., 2015;
488 Zhou et al., 2009) and with low values under low SWC (Reichstein et al., 2003; Tang et al., 2005). This is
489 also consistent with soil warming experiments by 0.76°C in Mediterranean ecosystems, which decreased
490 the R_s by 16%, and Q_{10} by 14% (Wang et al., 2014). Note also that the low temperature sensitivity in the
491 dry season is likely to be related to reduced microbial activity, but may also involve downregulation of
492 plant activity (Maseyk et al., 2008a) and drought-induced dormancy of shallow roots (Schiller, 2000).
493 Finally, we also note that the greater importance of moisture availability in influencing respiration is clearly
494 apparent from the observed relationships of R_s and R_h to mean annual precipitation (MAP) in European
495 evergreen needle forests (SI Fig. 8; see also Grünzweig et al., 2007), which are not observed with respect
496 to mean annual temperature.

497 ***Data availability***

498 The data used in this study are archived and available from the corresponding author upon request
499 (dan.yakir@weizmann.ac.il).

500 ***Author contributions***

501 RQ and DY designed the study; RQ, FT, ER and DY performed the experiments. RQ and DY analyzed the
502 data. DY and RQ wrote the paper, with discussions and contributions to interpretations of the results from
503 all co-authors.

504 ***Competing interests***

505 The authors declare that they have no conflict of interest.

506 **5. Acknowledgements**

507 This long-term study was funded by the Forestry Department of Keren-Kayemeth-LeIsrael (KKL) and the
508 German Research Foundation (DFG) as part of the project “Climate feedback and benefits of semi-arid
509 forests” (CliFF) and by the Israel Ministry of Science and the Ministry of National Education, Higher
510 Education, and Research (MENESR) of France (IMOS-French Program: 3-6735). The authors thank Efrat
511 Schwartz for assistance with lab work. The long-term operation of the Yatir Forest Research Field Site is
512 supported by the Cathy Wills and Robert Lewis Program in Environmental Science. We thank the entire
513 Yatir team for technical support and the local KKL personnel for their cooperation.

514 **6. References**

- 515
516 Adachi, M., Ito, A., Yonemura, S., and Takeuchi, W.: Estimation of global soil respiration by accounting for land-
517 use changes derived from remote sensing data, *Journal of Environmental Management*, 200, 97-104,
518 10.1016/j.jenvman.2017.05.076, 2017.
- 519 Angert, A., Yakir, D., Rodeghiero, M., Preisler, Y., Davidson, E. A., and Weiner, T.: Using O-2 to study the
520 relationships between soil CO₂ efflux and soil respiration, *Biogeosciences*, 12, 2089-2099, 10.5194/bg-12-2089-
521 2015, 2015.
- 522 Aubinet, M., Grelle, A., Ibrom, A., Rannik, U., Moncrieff, J., Foken, T., Kowalski, A. S., Martin, P. H., Berbigier,
523 P., Bernhofer, C., Clement, R., Elbers, J., Granier, A., Grunwald, T., Morgenstern, K., Pilegaard, K., Rebmann,
524 C., Snijders, W., Valentini, R., and Vesala, T.: Estimates of the annual net carbon and water exchange of forests:
525 The EUROFLUX methodology, *Advances in Ecological Research*, Vol 30, 30, 113-175, 2000.
- 526 Bahn, M., Janssens, I. A., Reichstein, M., Smith, P., and Trumbore, S. E.: Soil respiration across scales: towards an
527 integration of patterns and processes, *New Phytologist*, 186, 292-296, 10.1111/j.1469-8137.2010.03237.x, 2010.
- 528 Balogh, J., Pinter, K., Foti, S., Cserhalmi, D., Papp, M., and Nagy, Z.: Dependence of soil respiration on soil moisture,
529 clay content, soil organic matter, and CO₂ uptake in dry grasslands, *Soil Biology & Biochemistry*, 43, 1006-
530 1013, 10.1016/j.soilbio.2011.01.017, 2011.
- 531 Binkley, D., Stape, J. L., Takahashi, E. N., and Ryan, M. G.: Tree-girdling to separate root and heterotrophic
532 respiration in two Eucalyptus stands in Brazil, *Oecologia*, 148, 447-454, 10.1007/s00442-006-0383-6, 2006.
- 533 Bonan, G. B.: *Ecological climatology : concepts and applications*, 2nd ed., ed., Cambridge : Cambridge University
534 Press, Cambridge, 2008.
- 535 Bond-Lamberty, B., and Thomson, A.: Temperature-associated increases in the global soil respiration record, *Nature*,
536 464, 579-U132, 10.1038/nature08930, 2010.
- 537 Buchmann, N.: Biotic and abiotic factors controlling soil respiration rates in *Picea abies* stands, *Soil Biology &*

538 Biochemistry, 32, 1625-1635, 10.1016/s0038-0717(00)00077-8, 2000.

539 Carbone, M. S., Winston, G. C., and Trumbore, S. E.: Soil respiration in perennial grass and shrub ecosystems:
540 Linking environmental controls with plant and microbial sources on seasonal and diel timescales, *Journal of*
541 *Geophysical Research-Biogeosciences*, 113, 10.1029/2007jg000611, 2008.

542 Carmi, I., Yakir, D., Yechieli, Y., Kronfeld, J., and Stiller, M.: VARIATIONS IN SOIL CO₂ CONCENTRATIONS
543 AND ISOTOPIC VALUES IN A SEMI-ARID REGION DUE TO BIOTIC AND ABIOTIC PROCESSES IN
544 THE UNSATURATED ZONE, *Radiocarbon*, 55, 932-942, 2013.

545 Carvalhais, N., Forkel, M., Khomik, M., Bellarby, J., Jung, M., Migliavacca, M., Mu, M. Q., Saatchi, S., Santoro,
546 M., Thurner, M., Weber, U., Ahrens, B., Beer, C., Cescatti, A., Randerson, J. T., and Reichstein, M.: Global
547 covariation of carbon turnover times with climate in terrestrial ecosystems, *Nature*, 514, 213-+,
548 10.1038/nature13731, 2014.

549 Casals, P., Lopez-Sangil, L., Carrara, A., Gimeno, C., and Nogues, S.: Autotrophic and heterotrophic contributions
550 to short-term soil CO₂ efflux following simulated summer precipitation pulses in a Mediterranean dehesa, *Global*
551 *Biogeochemical Cycles*, 25, 10.1029/2010gb003973, 2011.

552 Chen, D., Zhang, Y., Lin, Y., Zhu, W., and Fu, S.: Changes in belowground carbon in *Acacia crassicarpa* and
553 *Eucalyptus urophylla* plantations after tree girdling, *Plant and Soil*, 326, 123-135, 10.1007/s11104-009-9986-0,
554 2010.

555 Chen, S. T., Zou, J. W., Hu, Z. H., Chen, H. S., and Lu, Y. Y.: Global annual soil respiration in relation to climate,
556 soil properties and vegetation characteristics: Summary of available data, *Agricultural and Forest Meteorology*,
557 198, 335-346, 10.1016/j.agrformet.2014.08.020, 2014.

558 Conant, R. T., Klopatek, J. M., Malin, R. C., and Klopatek, C. C.: Carbon pools and fluxes along an environmental
559 gradient in northern Arizona, *Biogeochemistry*, 43, 43-61, 10.1023/a:1006004110637, 1998.

560 Correia, A. C., Minunno, F., Caldeira, M. C., Banza, J., Mateus, J., Carneiro, M., Wingate, L., Shvaleyeva, A., Ramos,
561 A., Jongen, M., Bugalho, M. N., Nogueira, C., Lecomte, X., and Pereira, J. S.: Soil water availability strongly
562 modulates soil CO₂ efflux in different Mediterranean ecosystems: Model calibration using the Bayesian
563 approach, *Agriculture Ecosystems & Environment*, 161, 88-100, 10.1016/j.agee.2012.07.025, 2012.

564 Davidson, E. A., and Janssens, I. A.: Temperature sensitivity of soil carbon decomposition and feedbacks to climate
565 change, *Nature*, 440, 165-173, 10.1038/nature04514, 2006.

566 DeLucia, E. H., Drake, J. E., Thomas, R. B., and Gonzalez-Meler, M.: Forest carbon use efficiency: is respiration a
567 constant fraction of gross primary production?, *Global Change Biology*, 13, 1157-1167, 10.1111/j.1365-
568 2486.2007.01365.x, 2007.

569 Deng, Q., Hui, D., Zhang, D., Zhou, G., Liu, J., Liu, S., Chu, G., and Li, J.: Effects of Precipitation Increase on Soil
570 Respiration: A Three-Year Field Experiment in Subtropical Forests in China, *Plos One*, 7,
571 10.1371/journal.pone.0041493, 2012.

572 Etzold, S., Ruehr, N. K., Zweifel, R., Dobbertin, M., Zingg, A., Pluess, P., Hasler, R., Eugster, W., and Buchmann,
573 N.: The Carbon Balance of Two Contrasting Mountain Forest Ecosystems in Switzerland: Similar Annual
574 Trends, but Seasonal Differences, *Ecosystems*, 14, 1289-1309, 10.1007/s10021-011-9481-3, 2011.

575 Etzold, S., Zweifel, R., Ruehr, N. K., Eugster, W., and Buchmann, N.: Long-term stem CO₂ concentration
576 measurements in Norway spruce in relation to biotic and abiotic factors, *New Phytologist*, 197, 1173-1184,
577 10.1111/nph.12115, 2013.

578 Falge, E., Baldocchi, D., Tenhunen, J., Aubinet, M., Bakwin, P., Berbigier, P., Bernhofer, C., Burba, G., Clement,
579 R., Davis, K. J., Elbers, J. A., Goldstein, A. H., Grelle, A., Granier, A., Guomundsson, J., Hollinger, D.,
580 Kowalski, A. S., Katul, G., Law, B. E., Malhi, Y., Meyers, T., Monson, R. K., Munger, J. W., Oechel, W., Paw,
581 K. T., Pilegaard, K., Rannik, U., Rebmann, C., Suyker, A., Valentini, R., Wilson, K., and Wofsy, S.: Seasonality
582 of ecosystem respiration and gross primary production as derived from FLUXNET measurements, *Agricultural*
583 *and Forest Meteorology*, 113, 53-74, 10.1016/s0168-1923(02)00102-8, 2002.

584 Flechard, C. R., Ibrom, A., Skiba, U. M., de Vries, W., van Oijen, M., Cameron, D. R., Dise, N. B., Korhonen, J. F.
585 J., Buchmann, N., Legout, A., Simpson, D., Sanz, M. J., Aubinet, M., Loustau, D., Montagnani, L., Neiryneck, J.,
586 Janssens, I. A., Pihlatie, M., Kiese, R., Siemens, J., Francez, A.-J., Augustin, J., Varlagin, A., Olejnik, J.,
587 Juszczak, R., Aurela, M., Chojnicki, B. H., Dämmgen, U., Djuricic, V., Drewer, J., Eugster, W., Fauvel, Y.,
588 Fowler, D., Frumau, A., Granier, A., Gross, P., Hamon, Y., Helfter, C., Hensen, A., Horváth, L., Kitzler, B.,
589 Kruijt, B., Kutsch, W. L., Lobo-do-Vale, R., Lohila, A., Longdoz, B., Marek, M. V., Matteucci, G., Mitosinkova,
590 M., Moreaux, V., Neftel, A., Ourcival, J.-M., Pilegaard, K., Pita, G., Sanz, F., Schjoerring, J. K., Sebastia, M.-
591 T., Tang, Y. S., Uggerud, H., Urbaniak, M., van Dijk, N., Vesala, T., Vidic, S., Vincke, C., Weidinger, T.,
592 Zechmeister-Boltenstern, S., Butterbach-Bahl, K., Nemitz, E., and Sutton, M. A.: Carbon / nitrogen interactions
593 in European forests and semi-natural vegetation. Part I: Fluxes and budgets of carbon, nitrogen and greenhouse
594 gases from ecosystem monitoring and modelling, *Biogeosciences Discuss.*, <https://doi.org/10.5194/bg-2019-333>,

- 595 in review, 2019a.
- 596 Flechard, C. R., van Oijen, M., Cameron, D. R., de Vries, W., Ibrom, A., Buchmann, N., Dise, N. B., Janssens, I. A.,
597 Neiryneck, J., Montagnani, L., Varlagin, A., Loustau, D., Legout, A., Ziemblińska, K., Aubinet, M., Aurela, M.,
598 Chojnicki, B. H., Drewer, J., Eugster, W., Francez, A.-J., Juszczak, R., Kitzler, B., Kutsch, W. L., Lohila, A.,
599 Longdoz, B., Matteucci, G., Moreaux, V., Neftel, A., Olejnik, J., Sanz, M. J., Siemens, J., Vesala, T., Vincke,
600 C., Nemitz, E., Zechmeister-Boltenstern, S., Butterbach-Bahl, K., Skiba, U. M., and Sutton, M. A.:
601 Carbon / nitrogen interactions in European forests and semi-natural vegetation. Part II: Untangling climatic,
602 edaphic, management and nitrogen deposition effects on carbon sequestration potentials, *Biogeosciences*
603 Discuss., <https://doi.org/10.5194/bg-2019-335>, in review, 2019b.
- 604 Frank, A. B., Liebig, M. A., and Hanson, J. D.: Soil carbon dioxide fluxes in northern semiarid grasslands, *Soil*
605 *Biology & Biochemistry*, 34, 1235-1241, 10.1016/s0038-0717(02)00062-7, 2002.
- 606 Frey, B., Hagedorn, F., and Giudici, F.: Effect of girdling on soil respiration and root composition in a sweet chestnut
607 forest, *Forest Ecology and Management*, 225, 271-277, 10.1016/j.foreco.2006.01.003, 2006.
- 608 Gelfand, I., Grünzweig, J. M., and Yakir, D.: Slowing of nitrogen cycling and increasing nitrogen use efficiency
609 following afforestation of semi-arid shrubland, *Oecologia*, 168, 563-575, 10.1007/s00442-011-2111-0, 2012.
- 610 Giardina, C. P., and Ryan, M. G.: Total belowground carbon allocation in a fast-growing Eucalyptus plantation
611 estimated using a carbon balance approach, *Ecosystems*, 5, 487-499, 10.1007/s10021-002-0130-8, 2002.
- 612 Graven, H. D., Guilderson, T. P., and Keeling, R. F.: Observations of radiocarbon in CO₂ at La Jolla, California,
613 USA 1992-2007: Analysis of the long-term trend, *Journal of Geophysical Research-Atmospheres*, 117,
614 10.1029/2011jd016533, 2012.
- 615 Grünzweig, J. M., Gelfand, I., Fried, Y., and Yakir, D.: Biogeochemical factors contributing to enhanced carbon
616 storage following afforestation of a semi-arid shrubland, *Biogeosciences*, 4, 891-904, 2007.
- 617 Grünzweig, J. M., Hemming, D., Maseyk, K., Lin, T., Rotenberg, E., Raz-Yaseef, N., Falloon, P. D., and Yakir, D.:
618 Water limitation to soil CO₂ efflux in a pine forest at the semiarid "timberline", *Journal of Geophysical Research-*
619 *Biogeosciences*, 114, 10.1029/2008jg000874, 2009.
- 620 Grünzweig, J. M., Lin, T., Rotenberg, E., Schwartz, A., and Yakir, D.: Carbon sequestration in arid-land forest,
621 *Global Change Biology*, 9, 791-799, 10.1046/j.1365-2486.2003.00612.x, 2003.
- 622 Hagedorn, F., Joseph, J., Peter, M., Luster, J., Pritsch, K., Geppert, U., Kerner, R., Molinier, V., Egli, S., Schaub, M.,
623 Liu, J. F., Li, M. H., Sever, K., Weiler, M., Siegwolf, R. T. W., Gessler, A., and Arend, M.: Recovery of trees
624 from drought depends on belowground sink control, *Nature Plants*, 2, 10.1038/nplants.2016.111, 2016.
- 625 Hashimoto, S., Carvalhais, N., Ito, A., Migliavacca, M., Nishina, K., and Reichstein, M.: Global spatiotemporal
626 distribution of soil respiration modeled using a global database, *Biogeosciences*, 12, 4121-4132, 10.5194/bg-12-
627 4121-2015, 2015.
- 628 Hemming, D., Yakir, D., Ambus, P., Aurela, M., Besson, C., Black, K., Buchmann, N., Burlett, R., Cescatti, A.,
629 Clement, R., Gross, P., Granier, A., Grunwald, T., Havrankova, K., Janous, D., Janssens, I. A., Knohl, A., Ostner,
630 B. K., Kowalski, A., Laurila, T., Mata, C., Marcolla, B., Matteucci, G., Moncrieff, J., Moors, E. J., Osborne, B.,
631 Pereira, J. S., Pihlatie, M., Pilegaard, K., Ponti, F., Rosova, Z., Rossi, F., Scartazza, A., and Vesala, T.: Pan-
632 European delta C-13 values of air and organic matter from forest ecosystems, *Global Change Biology*, 11, 1065-
633 1093, 10.1111/j.1365-2486.2005.00971.x, 2005.
- 634 Hogberg, P., Bhupinderpal, S., Lofvenius, M. O., and Nordgren, A.: Partitioning of soil respiration into its autotrophic
635 and heterotrophic components by means of tree-girdling in old boreal spruce forest, *Forest Ecology and*
636 *Management*, 257, 1764-1767, 10.1016/j.foreco.2009.01.036, 2009.
- 637 Hui, D. F., and Luo, Y. Q.: Evaluation of soil CO₂ production and transport in Duke Forest using a process-based
638 modeling approach, *Global Biogeochemical Cycles*, 18, 10.1029/2004gb002297, 2004.
- 639 IPCC. Climate Change 2014: Mitigation of Climate Change. Contribution of Working Group III to the Fifth
640 Assessment Report of the Intergovernmental Panel on Climate Change [Edenhofer, O., R. et al.]. Cambridge
641 University Press, Cambridge and New York, 2014.
- 642 Jiang, H., Deng, Q., Zhou, G., Hui, D., Zhang, D., Liu, S., Chu, G., and Li, J.: Responses of soil respiration and its
643 temperature/moisture sensitivity to precipitation in three subtropical forests in southern China, *Biogeosciences*,
644 10, 3963-3982, 10.5194/bg-10-3963-2013, 2013.
- 645 Joseph, J., Kulls, C., Arend, M., Schaub, M., Hagedorn, F., Gessler, A., and Weiler, M.: Application of a laser-based
646 spectrometer for continuous in situ measurements of stable isotopes of soil CO₂ in calcareous and acidic soils,
647 *Soil*, 5, 49-62, 10.5194/soil-5-49-2019, 2019.
- 648 Kool, D. M., Chung, H. G., Tate, K. R., Ross, D. J., Newton, P. C. D., and Six, J.: Hierarchical saturation of soil
649 carbon pools near a natural CO₂ spring, *Global Change Biology*, 13, 1282-1293, 10.1111/j.1365-
650 2486.2007.01362.x, 2007.
- 651 Kowalski, A. S., Serrano-Ortiz, P., Janssens, I. A., Sanchez-Moral, S., Cuezva, S., Domingo, F., Were, A., and

652 Alados-Arboledas, L.: Can flux tower research neglect geochemical CO₂ exchange?, *Agricultural and Forest*
653 *Meteorology*, 148, 1045-1054, 10.1016/j.agrformet.2008.02.004, 2008.

654 Kuzyakov, Y.: Sources of CO₂ efflux from soil and review of partitioning methods, *Soil Biology & Biochemistry*,
655 38, 425-448, 10.1016/j.soilbio.2005.08.020, 2006.

656 Lelieveld, J., Hadjinicolaou, P., Kostopoulou, E., Chenoweth, J., El Maayar, M., Giannakopoulos, C., Hannides, C.,
657 Lange, M. A., Tanarhte, M., Tyrllis, E., and Xoplaki, E.: Climate change and impacts in the Eastern Mediterranean
658 and the Middle East, *Climatic Change*, 114, 667-687, 10.1007/s10584-012-0418-4, 2012.

659 Lellei-Kovacs, E., Kovacs-Lang, E., Botta-Dukat, Z., Kalapos, T., Emmett, B., and Beier, C.: Thresholds and
660 interactive effects of soil moisture on the temperature response of soil respiration, *European Journal of Soil*
661 *Biology*, 47, 247-255, 10.1016/j.ejsobi.2011.05.004, 2011.

662 Levin, I., Naegler, T., Kromer, B., Diehl, M., Francey, R. J., Gomez-Pelaez, A. J., Steele, L. P., Wagenbach, D.,
663 Weller, R., and Worthy, D. E.: Observations and modelling of the global distribution and long-term trend of
664 atmospheric (CO₂)-C-14 (vol 62, pg 26, 2010), *Tellus Series B-Chemical and Physical Meteorology*, 62, 207-
665 207, 10.1111/j.1600-0889.2010.00456.x, 2010.

666 Lin, G. H., Ehleringer, J. R., Rygielwicz, P. T., Johnson, M. G., and Tingey, D. T.: Elevated CO₂ and temperature
667 impacts on different components of soil CO₂ efflux in Douglas-fir terracosms, *Global Change Biology*, 5, 157-
668 168, 10.1046/j.1365-2486.1999.00211.x, 1999.

669 Litton, C. M., Raich, J. W., and Ryan, M. G.: Carbon allocation in forest ecosystems, *Global Change Biology*, 13,
670 2089-2109, 10.1111/j.1365-2486.2007.01420.x, 2007.

671 Lopez-Ballesteros, A., Serrano-Ortiz, P., Kowalski, A. S., Sanchez-Canete, E. P., Scott, R. L., and Domingo, F.:
672 Subterranean ventilation of allochthonous CO₂ governs net CO₂ exchange in a semiarid Mediterranean
673 grassland, *Agricultural and Forest Meteorology*, 234, 115-126, 10.1016/j.agrformet.2016.12.021, 2017.

674 Luyssaert, S., Inglima, I., Jung, M., Richardson, A. D., Reichstein, M., Papale, D., Piao, S. L., Schulzes, E. D.,
675 Wingate, L., Matteucci, G., Aragao, L., Aubinet, M., Beers, C., Bernhofer, C., Black, K. G., Bonal, D.,
676 Bonnefond, J. M., Chambers, J., Ciais, P., Cook, B., Davis, K. J., Dolman, A. J., Gielen, B., Goulden, M., Grace,
677 J., Granier, A., Grelle, A., Griffis, T., Grunwald, T., Guidolotti, G., Hanson, P. J., Harding, R., Hollinger, D. Y.,
678 Hutrya, L. R., Kolar, P., Kruijt, B., Kutsch, W., Lagergren, F., Laurila, T., Law, B. E., Le Maire, G., Lindroth,
679 A., Loustau, D., Malhi, Y., Mateus, J., Migliavacca, M., Misson, L., Montagnani, L., Moncrieff, J., Moors, E.,
680 Munger, J. W., Nikinmaa, E., Ollinger, S. V., Pita, G., Rebmann, C., Rouspard, O., Saigusa, N., Sanz, M. J.,
681 Seufert, G., Sierra, C., Smith, M. L., Tang, J., Valentini, R., Vesala, T., and Janssens, I. A.: CO₂ balance of
682 boreal, temperate, and tropical forests derived from a global database, *Global Change Biology*, 13, 2509-2537,
683 10.1111/j.1365-2486.2007.01439.x, 2007.

684 Maseyk, K., Grünzweig, J. M., Rotenberg, E., and Yakir, D.: Respiration acclimation contributes to high carbon-use
685 efficiency in a seasonally dry pine forest, *Global Change Biology*, 14, 1553-1567, 10.1111/j.1365-
686 2486.2008.01604.x, 2008a.

687 Matteucci, M., Gruening, C., Ballarin, I. G., Seufert, G., and Cescatti, A.: Components, drivers and temporal
688 dynamics of ecosystem respiration in a Mediterranean pine forest, *Soil Biology & Biochemistry*, 88, 224-235,
689 10.1016/j.soilbio.2015.05.017, 2015.

690 Misson, L., Rocheteau, A., Rambal, S., Ourcival, J. M., Limousin, J. M., and Rodriguez, R.: Functional changes in
691 the control of carbon fluxes after 3 years of increased drought in a Mediterranean evergreen forest?, *Global*
692 *Change Biology*, 16, 2461-2475, 10.1111/j.1365-2486.2009.02121.x, 2010.

693 Pataki, D. E., Ehleringer, J. R., Flanagan, L. B., Yakir, D., Bowling, D. R., Still, C. J., Buchmann, N., Kaplan, J. O.,
694 and Berry, J. A.: The application and interpretation of Keeling plots in terrestrial carbon cycle research, *Global*
695 *Biogeochemical Cycles*, 17, 10.1029/2001gb001850, 2003.

696 Peterjohn, W. T., Melillo, J. M., Steudler, P. A., Newkirk, K. M., Bowles, F. P., and Aber, J. D.: RESPONSES OF
697 TRACE GAS FLUXES AND N AVAILABILITY TO EXPERIMENTALLY ELEVATED SOIL
698 TEMPERATURES, *Ecological Applications*, 4, 617-625, 10.2307/1941962, 1994.

699 Poulter, B., Frank, D., Ciais, P., Myneni, R. B., Andela, N., Bi, J., Broquet, G., Canadell, J. G., Chevallier, F., Liu,
700 Y. Y., Running, S. W., Sitch, S., and van der Werf, G. R.: Contribution of semi-arid ecosystems to interannual
701 variability of the global carbon cycle, *Nature*, 509, 600-+, 10.1038/nature13376, 2014.

702 Preisler, Y., Tatarinov, F., Grunzweig, J. M., Bert, D., Ogee, J., Wingate, L., Rotenberg, E., Rohatyn, S., Her, N.,
703 Moshe, I., Klein, T., and Yakir, D.: Mortality versus survival in drought-affected Aleppo pine forest depends on
704 the extent of rock cover and soil stoniness, *Functional Ecology*, 33, 901-912, 10.1111/1365-2435.13302, 2019.

705 Qubaja, R., Grünzweig, J., Rotenberg, E., and Yakir, D.: Evidence for large carbon sink and long residence time in
706 semiarid forests based on 15 year flux and inventory records. *Global Change Biology*, 10.1111/gcb.14927, 2019.

707 Raich, J. W., and Schlesinger, W. H.: THE GLOBAL CARBON-DIOXIDE FLUX IN SOIL RESPIRATION AND
708 ITS RELATIONSHIP TO VEGETATION AND CLIMATE, *Tellus Series B-Chemical and Physical*

709 Meteorology, 44, 81-99, 10.1034/j.1600-0889.1992.t01-1-00001.x, 1992.

710 Ramnarine, R., Wagner-Riddle, C., Dunfield, K. E., and Voroney, R. P.: Contributions of carbonates to soil CO₂

711 emissions, Canadian Journal of Soil Science, 92, 599-607, 10.4141/cjss2011-025, 2012.

712 Raz-Yaseef, N., Rotenberg, E., and Yakir, D.: Effects of spatial variations in soil evaporation caused by tree shading

713 on water flux partitioning in a semi-arid pine forest, Agricultural and Forest Meteorology, 150, 454-462,

714 10.1016/j.agrformet.2010.01.010, 2010.

715 Reichstein, M., Rey, A., Freibauer, A., Tenhunen, J., Valentini, R., Banza, J., Casals, P., Cheng, Y. F., Grünzweig,

716 J. M., Irvine, J., Joffre, R., Law, B. E., Loustau, D., Miglietta, F., Oechel, W., Ourcival, J. M., Pereira, J. S.,

717 Peressotti, A., Ponti, F., Qi, Y., Rambal, S., Rayment, M., Romanya, J., Rossi, F., Tedeschi, V., Tirone, G., Xu,

718 M., and Yakir, D.: Modeling temporal and large-scale spatial variability of soil respiration from soil water

719 availability, temperature and vegetation productivity indices, Global Biogeochemical Cycles, 17,

720 10.1029/2003gb002035, 2003.

721 Rey, A., Pegoraro, E., Tedeschi, V., De Parri, I., Jarvis, P. G., and Valentini, R.: Annual variation in soil respiration

722 and its components in a coppice oak forest in Central Italy, Global Change Biology, 8, 851-866, 10.1046/j.1365-

723 2486.2002.00521.x, 2002.

724 Rodeghiero, M., and Cescatti, A.: Main determinants of forest soil respiration along an elevation/temperature gradient

725 in the Italian Alps, Global Change Biology, 11, 1024-1041, 10.1111/j.1365-2486.2005.00963.x, 2005.

726 Roland, M.: Contributions of carbonate weathering to the net ecosystem carbon balance of a mediterranean forest,

727 Ph.D. thesis, Antwerpen University, Antwerpen, Belgium, 2012.

728 Ross, I., Misson, L., Rambal, S., Arneth, A., Scott, R. L., Carrara, A., Cescatti, A., and Genesio, L.: How do variations

729 in the temporal distribution of rainfall events affect ecosystem fluxes in seasonally water-limited Northern

730 Hemisphere shrublands and forests?, Biogeosciences, 9, 1007-1024, 10.5194/bg-9-1007-2012, 2012.

731 Rotenberg, E., and Yakir, D.: Contribution of Semi-Arid Forests to the Climate System, Science, 327, 451-454,

732 10.1126/science.1179998, 2010.

733 Schiller, G.: Ecophysiology of *Pinus halepensis* Mill. and *P. brutia* Ten, in Ecology, Biogeography and Management

734 of *Pinus halepensis* and *P. brutia* Forest Ecosystems in the Mediterranean Basin, edited by: Ne'eman, G., and

735 Trabaud, L., Backhuys, Leiden, Netherlands, 51-65, 2000.

736 Serrano-Ortiz, P., Roland, M., Sanchez-Moral, S., Janssens, I. A., Domingo, F., Godderis, Y., and Kowalski, A. S.:

737 Hidden, abiotic CO₂ flows and gaseous reservoirs in the terrestrial carbon cycle: Review and perspectives,

738 Agricultural and Forest Meteorology, 150, 321-329, 10.1016/j.agrformet.2010.01.002, 2010.

739 Shachnovich, Y., Berliner, P. R., and Bar, P.: Rainfall interception and spatial distribution of throughfall in a pine

740 forest planted in an arid zone, Journal of Hydrology, 349, 168-177, 10.1016/j.jhydrol.2007.10.051, 2008.

741 Shen, W. J., Jenerette, G. D., Hui, D. F., Phillips, R. P., and Ren, H.: Effects of changing precipitation regimes on

742 dryland soil respiration and C pool dynamics at rainfall event, seasonal and interannual scales, Journal of

743 Geophysical Research-Biogeosciences, 113, 10.1029/2008jg000685, 2008.

744 Subke, J.-A., Voke, N. R., Leronni, V., Garnett, M. H., and Ineson, P.: Dynamics and pathways of autotrophic and

745 heterotrophic soil CO₂ efflux revealed by forest girdling, Journal of Ecology, 99, 186-193, 10.1111/j.1365-

746 2745.2010.01740.x, 2011.

747 Taneva, L., and Gonzalez-Meler, M. A.: Distinct patterns in the diurnal and seasonal variability in four components

748 of soil respiration in a temperate forest under free-air CO₂ enrichment, Biogeosciences, 8, 3077-3092,

749 10.5194/bg-8-3077-2011, 2011.

750 Tang, J. W., Baldocchi, D. D., and Xu, L.: Tree photosynthesis modulates soil respiration on a diurnal time scale,

751 Global Change Biology, 11, 1298-1304, 10.1111/j.1365-2486.2005.00987.x, 2005.

752 Tatarinov, F., Rotenberg, E., Maseyk, K., Ogee, J., Klein, T., and Yakir, D.: Resilience to seasonal heat wave episodes

753 in a Mediterranean pine forest, New Phytologist, 210, 485-496, 10.1111/nph.13791, 2016.

754 Taylor, A. J., Lai, C. T., Hopkins, F. M., Wharton, S., Bible, K., Xu, X. M., Phillips, C., Bush, S., and Ehleringer, J.

755 R.: Radiocarbon-Based Partitioning of Soil Respiration in an Old-Growth Coniferous Forest, Ecosystems, 18,

756 459-470, 10.1007/s10021-014-9839-4, 2015.

757 Volcani, A., Karnieli, A., and Svoray, T.: The use of remote sensing and GIS for spatio-temporal analysis of the

758 physiological state of a semi-arid forest with respect to drought years, Forest Ecology and Management, 215,

759 239-250, 10.1016/j.foreco.2005.05.063, 2005.

760 Wang, X., Liu, L. L., Piao, S. L., Janssens, I. A., Tang, J. W., Liu, W. X., Chi, Y. G., Wang, J., and Xu, S.: Soil

761 respiration under climate warming: differential response of heterotrophic and autotrophic respiration, Global

762 Change Biology, 20, 3229-3237, 10.1111/gcb.12620, 2014b.

763 Xu, M., and Qi, Y.: Soil-surface CO₂ efflux and its spatial and temporal variations in a young ponderosa pine

764 plantation in northern California, Global Change Biology, 7, 667-677, 10.1046/j.1354-1013.2001.00435.x, 2001.

765 Xu, Z. F., Tang, S. S., Xiong, L., Yang, W. Q., Yin, H. J., Tu, L. H., Wu, F. Z., Chen, L. H., and Tan, B.: Temperature

766 sensitivity of soil respiration in China's forest ecosystems: Patterns and controls, *Applied Soil Ecology*, 93, 105-
767 110, 10.1016/j.apsoil.2015.04.008, 2015.

768 Yu, S. Q., Chen, Y. Q., Zhao, J., Fu, S. L., Li, Z., Xia, H. P., and Zhou, L. X.: Temperature sensitivity of total soil
769 respiration and its heterotrophic and autotrophic components in six vegetation types of subtropical China, *Science*
770 *of the Total Environment*, 607, 160-167, 10.1016/j.scitotenv.2017.06.194, 2017a.

771 Zhou, T., Shi, P. J., Hui, D. F., and Luo, Y. Q.: Global pattern of temperature sensitivity of soil heterotrophic
772 respiration (Q(10)) and its implications for carbon-climate feedback, *Journal of Geophysical Research-*
773 *Biogeosciences*, 114, 10.1029/2008jg000850, 2009.